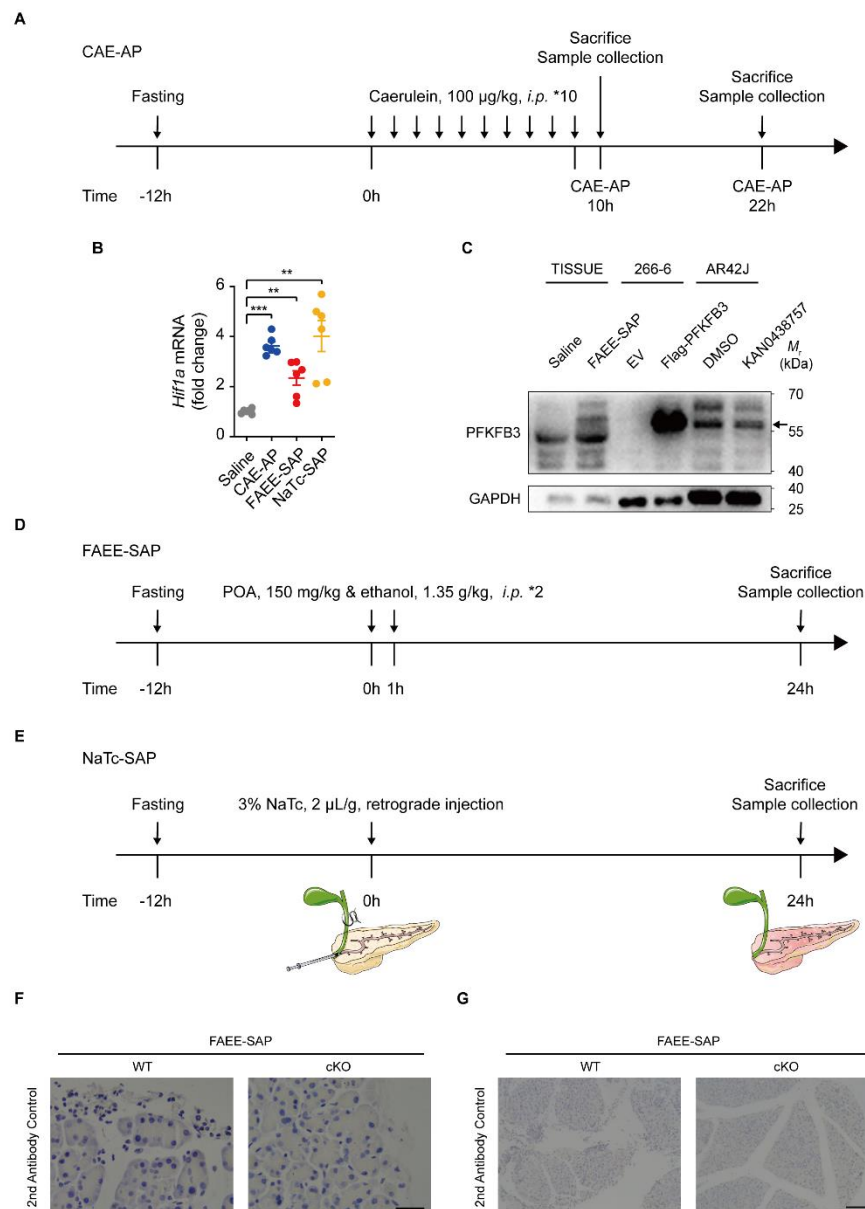
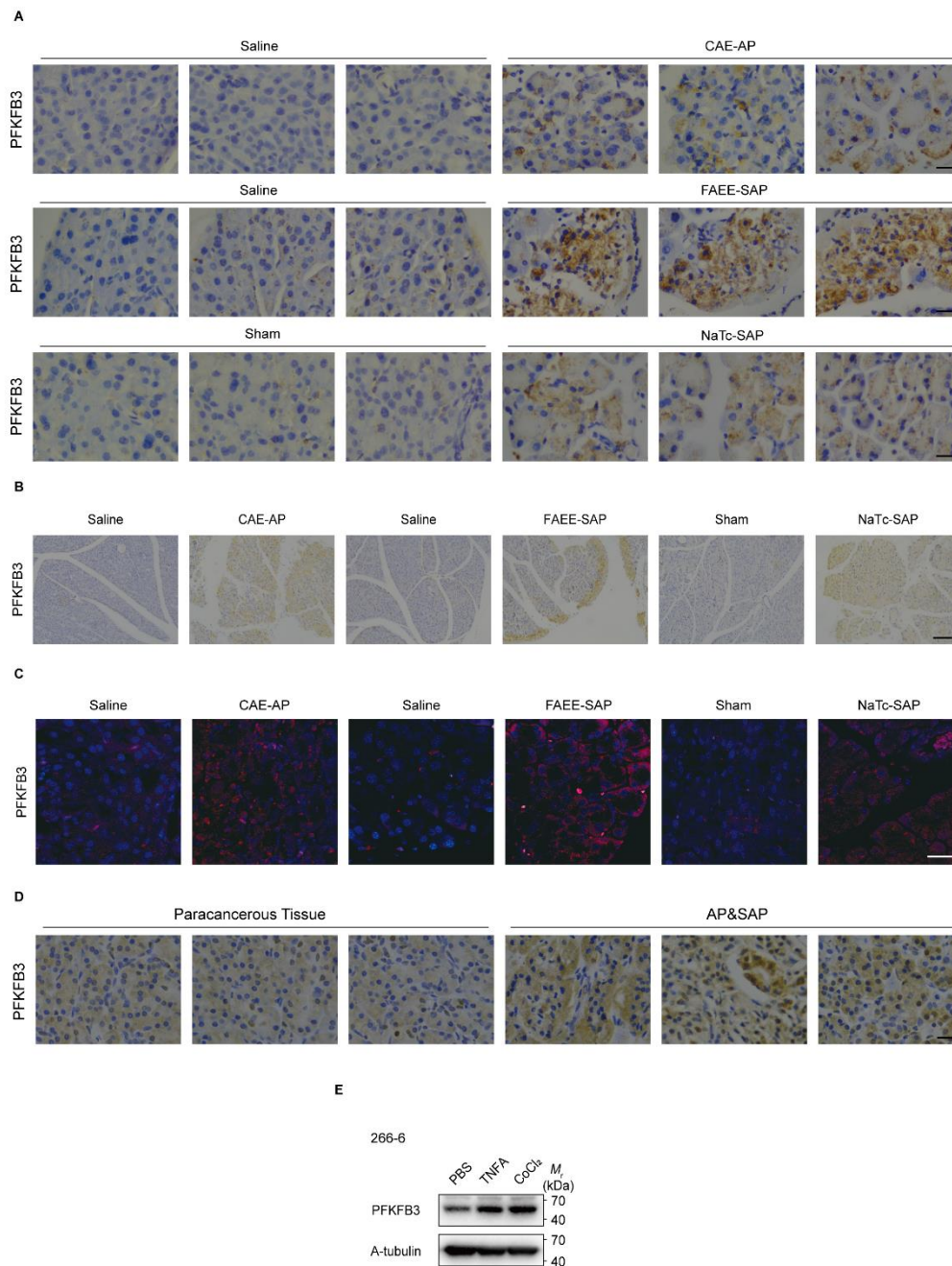


## Supplementary materials

Tan Z. et al.Fig.S1



**Figure S1. Schematic diagram of the CAE-AP, FAEE-SAP and NaTc-SAP mouse model. (A)** Schematic diagram of the CAE-AP mouse. **(B)** The relative transcription level of *Hif1a* was measured using RT-qPCR in pancreas collected from CAE-AP, FAEE-SAP, NaTc-SAP and control mice (n=6). **(C)** The protein from pancreatic tissue, 266-6 cells and AR42J cells were collected for Western blotting analysis. **(D)** Schematic diagram of the FAEE-SAP mouse model. **(E)** Schematic diagram of the NaTc-SAP mouse model. **(F-G)** The secondary antibody control of PFKFB3 IHC analysis, scale bar, 30µm **(F)** and 200µm **(G)**. Statistical analyses were done using one-way ANOVA test and shown as mean ± SD, \*\*p<0.01, \*\*\*p<0.001. Each experiment was done at least in triplicate.



**Figure S2. PFKFB3 is upregulated of AP and SAP.** (A) Immunohistochemical analysis of PFKFB3 in pancreas from control group (n=5) and CAE-AP, FAEE-SAP and NaTc-SAP models (n=5), scale bar, 100µm. (B) Low magnification images of IHC stain in 3 AP models, scale bar, 200µm. (C) Immunofluorescence analysis of PFKFB3 in pancreas from control group and CAE-AP, FAEE-SAP and NaTc-SAP models, scale bar, 50µm. (D) Immunohistochemical analysis of PFKFB3 in pancreas from AP & SAP patient (n=5), scale bar, 40µm. (E) PFKFB3 levels were detected using Western blotting in 266-6 cells treated with TNFA (40ng/ml; 24h) and CoCl<sub>2</sub> (200µmol/l;24h). Each experiment was done at least in triplicate.

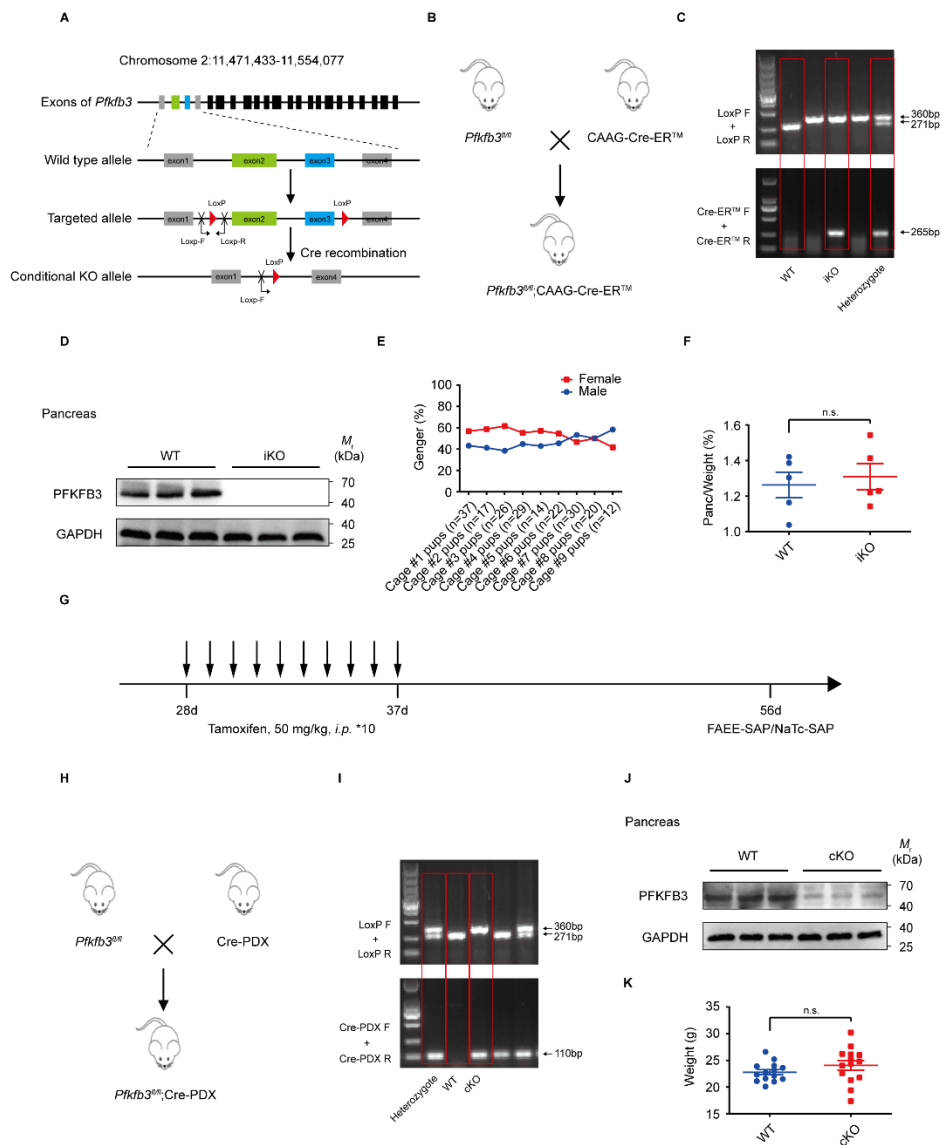


**Figure S3. Development of *Pfkfb3* inducible knockout (iKO) and conditional knockout (cKO) mice models.** (A) Strategy of Cre-LoxP recombination for the *Pfkfb3* knockout in C57BL/6cnc mice. (B) Breeding scheme of iKO mice. (C) Representative genotyping example of iKO mice. (D) The western blotting assay was used to verified the *Pfkfb3* knockout state in iKO mice in physiological status. (E) Gender distribution of iKO mice in multiple generations (n=9). (F) The ratio of pancreatic weight to body weight of iKO mice at 8 weeks compared to the WT counterpart (n=5). (G) Induction scheme for inducible *Pfkfb3* knockout. (H) Breeding scheme of cKO mice. (I) Representative genotyping example of cKO mice. (J) The western blotting assay was used to verified the *Pfkfb3* knockout state in cKO mice in physiological status. (K) Body weight in grams (g) of cKO mice at 8 weeks compared to the WT counterparts (n=14). Statistical analyses were done using unpaired student t-test and shown as mean  $\pm$  SD, n.s., not significant.

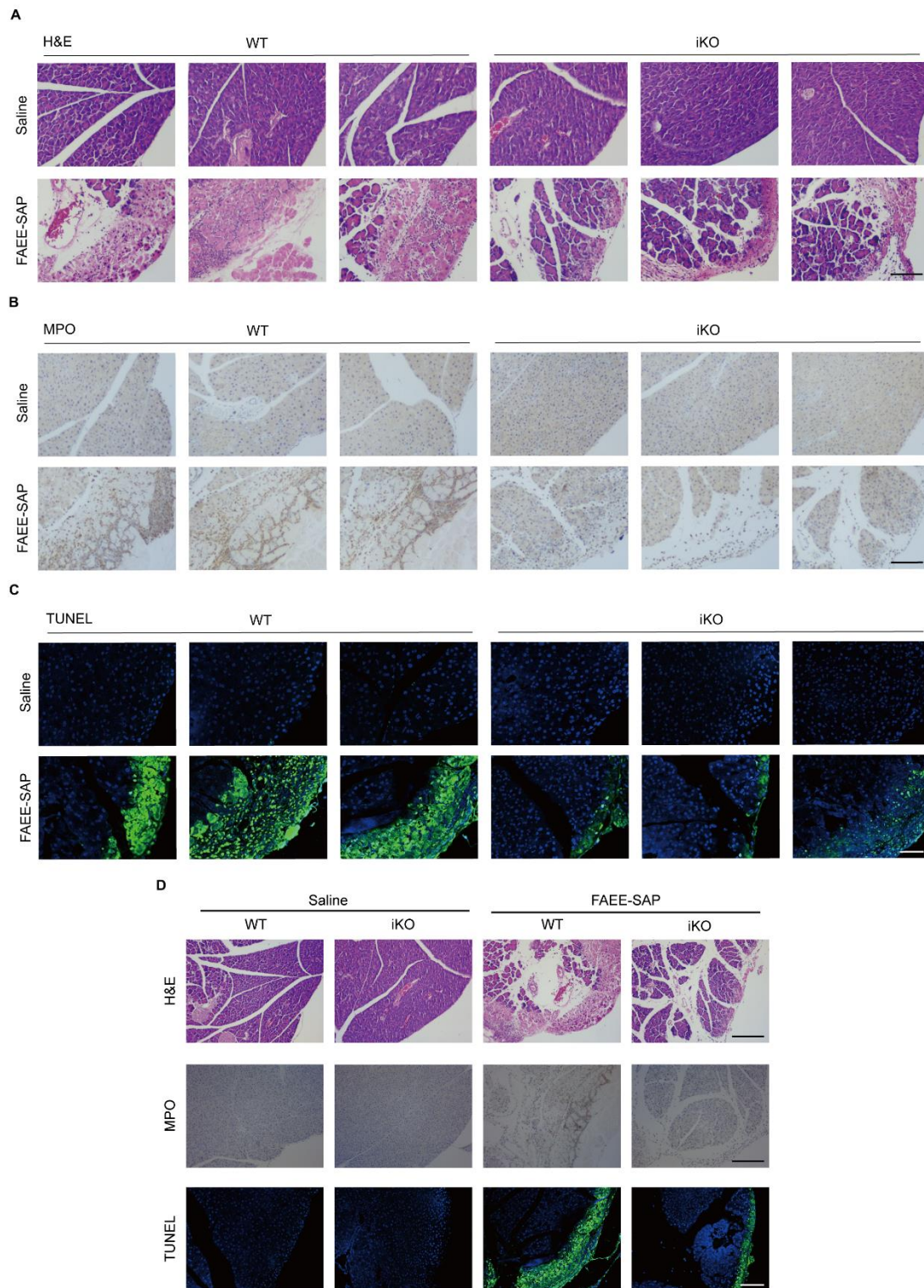


**Figure S4. H&E (A), MPO (B), and TUNEL (C) staining of injured and normal pancreas in WT mice and iKO mice. Scale bar, 100µm. (D) Low magnification images of H&E, MPO and TUNEL stains of injured and normal pancreas in WT mice and iKO mice. Scale bar, 200µm.**

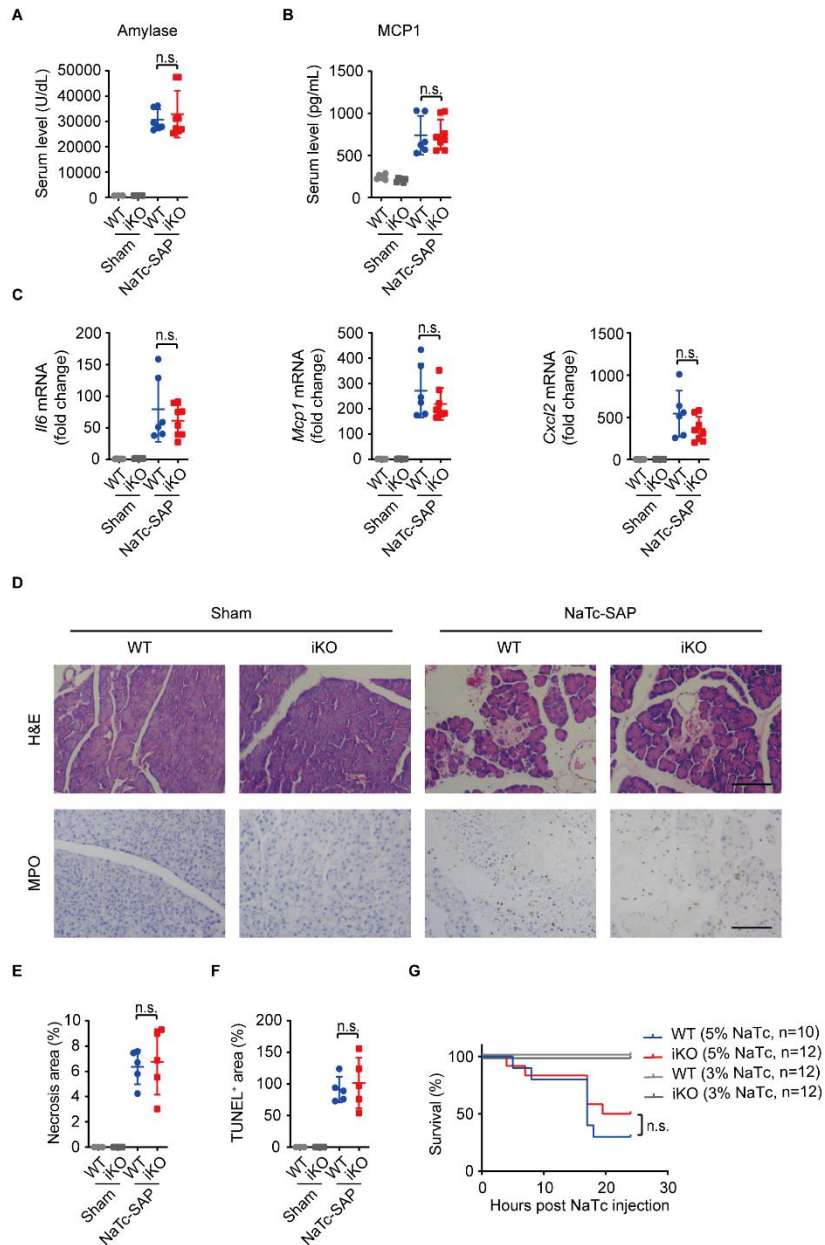


**Figure S5. The inducible knockout (iKO) mice do not affect pancreatitis severity in the NaTc-SAP model. (A-B)** Serum amylase (A) and MCP1 (B) levels were evaluated using iodine-starch colorimetry and ELISA in iKO and WT control mice from the NaTc-SAP (n=3-8). **(C)** The relative mRNA expression of inflammatory genes, *Il6*, *Mcp1* and *Cxcl2* were measured using RT-qPCR in pancreas from iKO and WT control mice in the NaTc-SAP model (n=6-8). **(D)** H&E and MPO staining in injured and control pancreas; scale bar, 200 $\mu$ m. **(E-F)** Quantification of levels necrosis (E) and MPO (F) (n=3-5). **(G)** Twenty-four hours survival of mice from the NaTc-SAP model (n=10-12). The statistical analysis of the survival was done using log-rank (Mantel-Cox) test, and all other statistical analyses were unpaired student t-test and shown as mean  $\pm$  SD, n.s., not significant. Each experiment was done at least in triplicate.

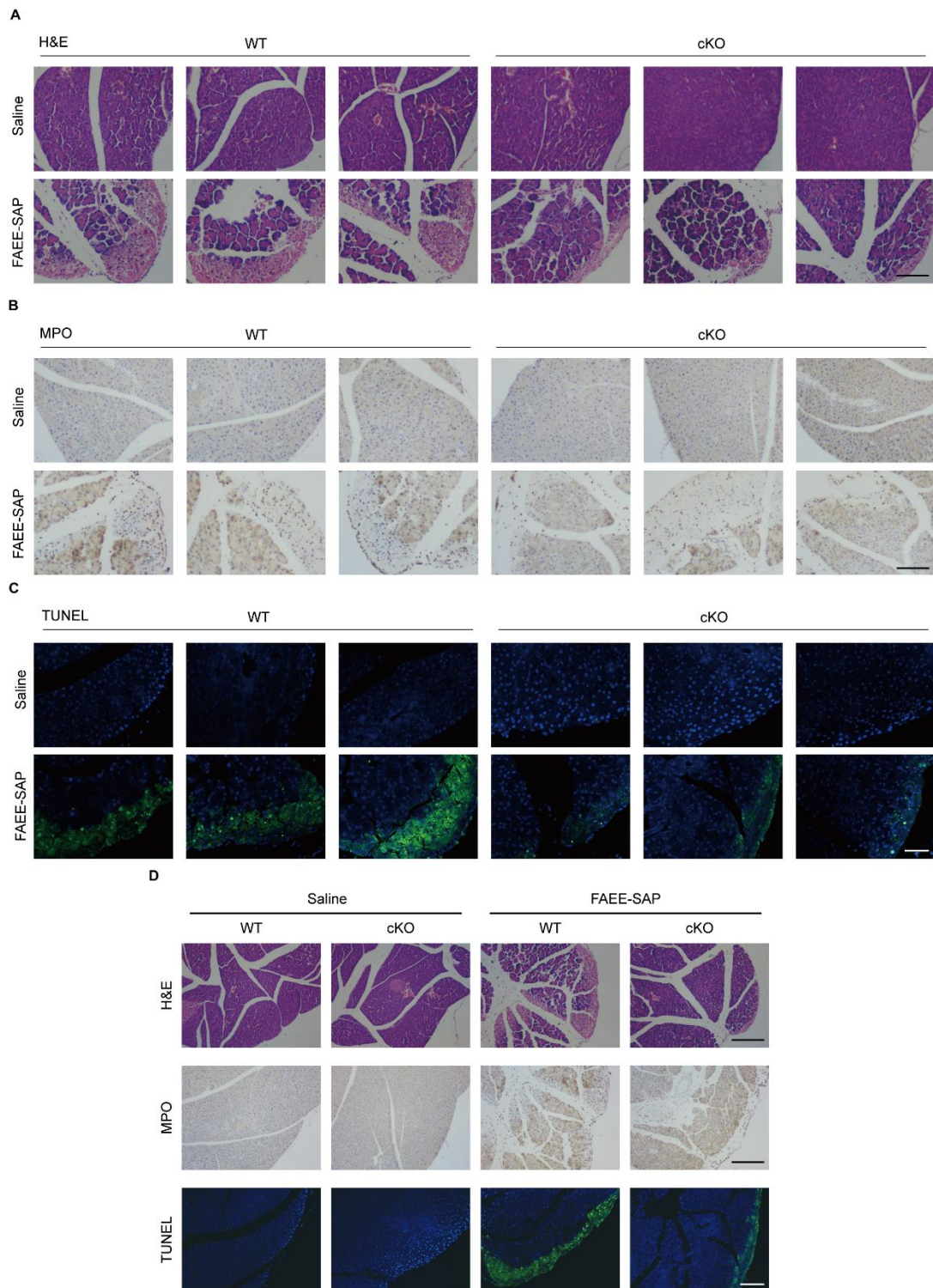


**Figure S6. H&E (A), MPO (B), and TUNEL (C) staining of injured and normal pancreas in WT mice and cKO mice. Scale bar, 100 $\mu$ m. (D) Low magnification images of H&E, MPO and TUNEL stains of injured and normal pancreas in WT mice and cKO mice. Scale bar, 200 $\mu$ m.**

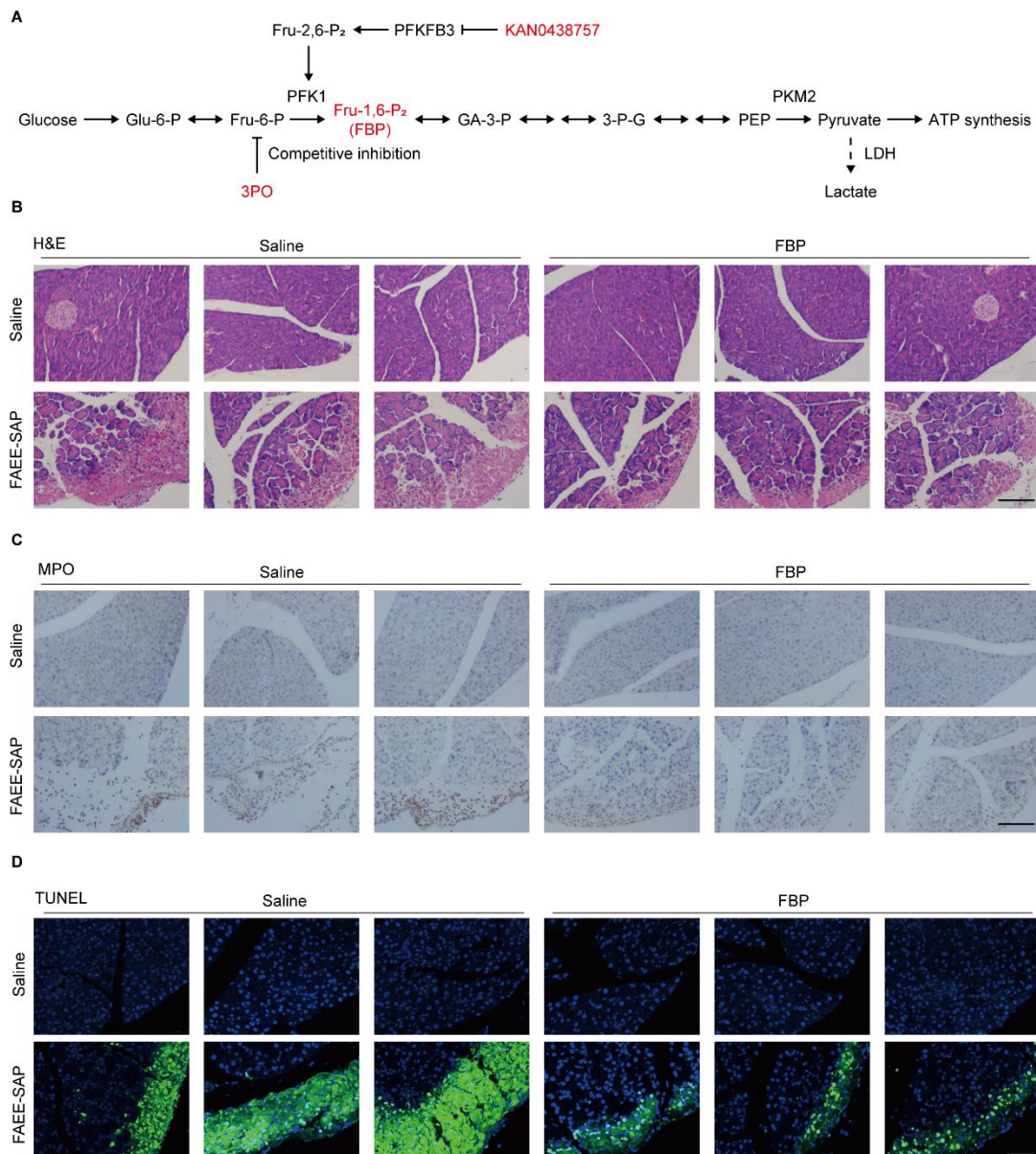


**Figure S7. FBP protect WT mice from FAEE-SAP.** (A) Working schematic of 3PO, FBP and KAN0438757 in glycolysis pathway. (B-D) H&E (B), MPO (C), and TUNEL (D) staining of injured and normal pancreas. Scale bar, 100µm. Each experiment was done at least in triplicate.

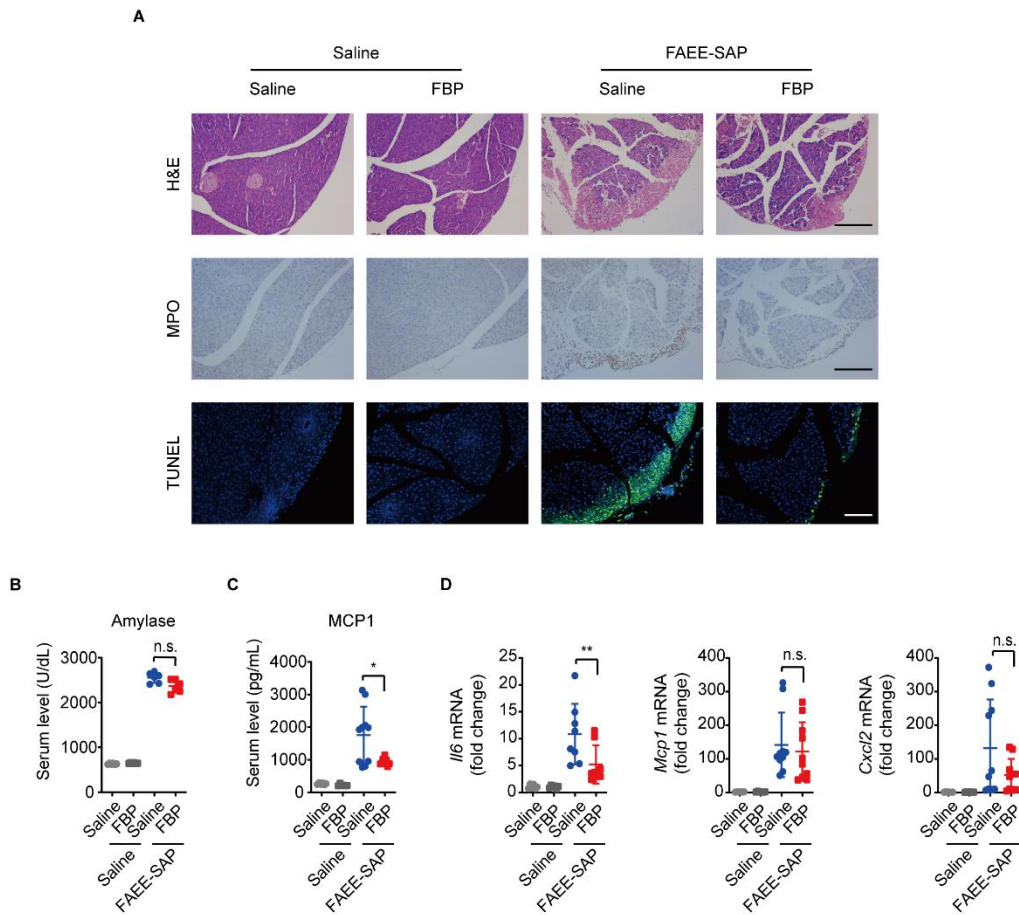


**Figure S8. FBP protect WT mice from FAEE-SAP.** (A) Low magnification images of H&E, MPO and TUNEL stains of injured and normal pancreas. Scale bar, 200 $\mu$ m. (B-C) Serum amylase (B) and MCP1 (C) levels were detected using Iodine-starch colorimetry and ELISA in FAEE-SAP and control mice (n=6-10). (D) *Il6*, *Mcp1* and *Cxcl2* mRNA expression were measured using RT-qPCR in pancreas collected from FAEE-SAP and control mice (n=6-10). Statistical analyses were done using unpaired student t-test and shown as mean  $\pm$  SD, \* $p$ <0.05, \*\* $p$ <0.01, \*\*\* $p$ <0.001. Each experiment was done at least in triplicate.



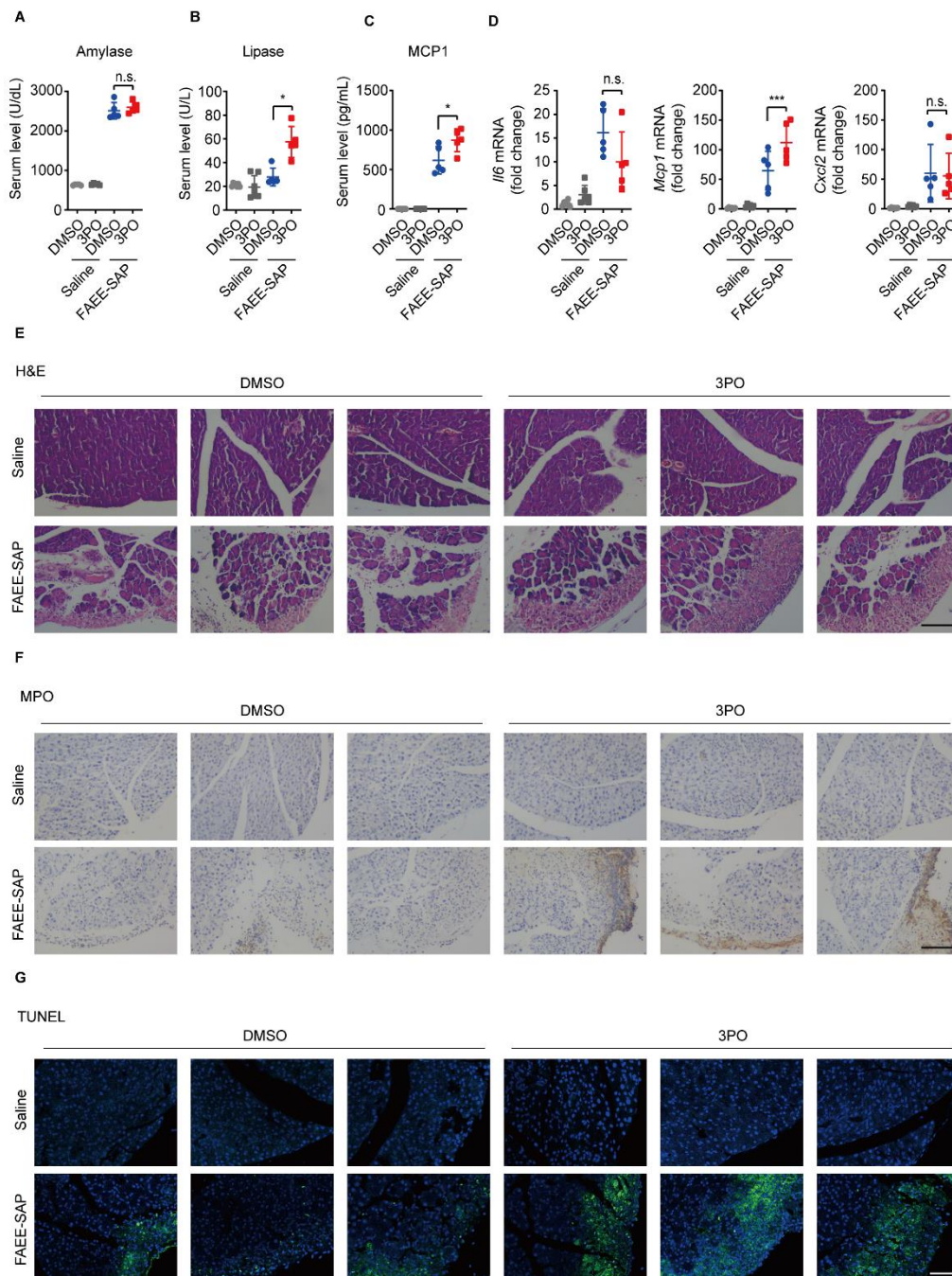


**Figure S9. 3PO aggravates the severity of FAEE-SAP.** (A-C) Serum amylase (A), lipase (B) and MCP1 (C) levels were detected using colorimetry and ELISA, respectively in FAEE-SAP and control mice (n=5-7). (D) Relative expression of inflammatory genes, *Il6*, *Mcp1* and *Cxcl2*, were measured using RT-qPCR in pancreas collected from FAEE-SAP and control mice (n=5-6). (E-G) H&E (E), MPO (F), and TUNEL (G) staining of injured and normal pancreas. Scale bar, 100 $\mu$ m. Statistical analyses were done using unpaired student t-test and shown as mean  $\pm$  SD, \* $p$ <0.05, \*\* $p$ <0.01, \*\*\* $p$ <0.001. Each experiment was done at least in triplicate.

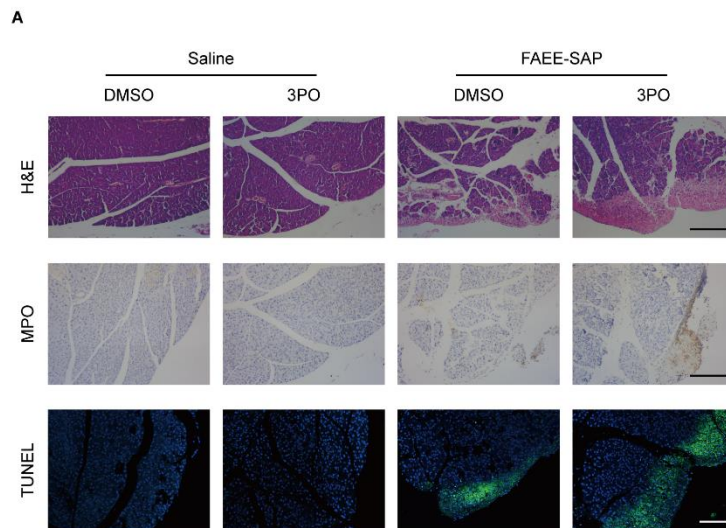


**Figure S10. 3PO aggravates the severity of FAEE-SAP. (A)** Low magnification images of H&E, MPO and TUNEL stains of injured and normal pancreas. Scale bar, 200 $\mu$ m.

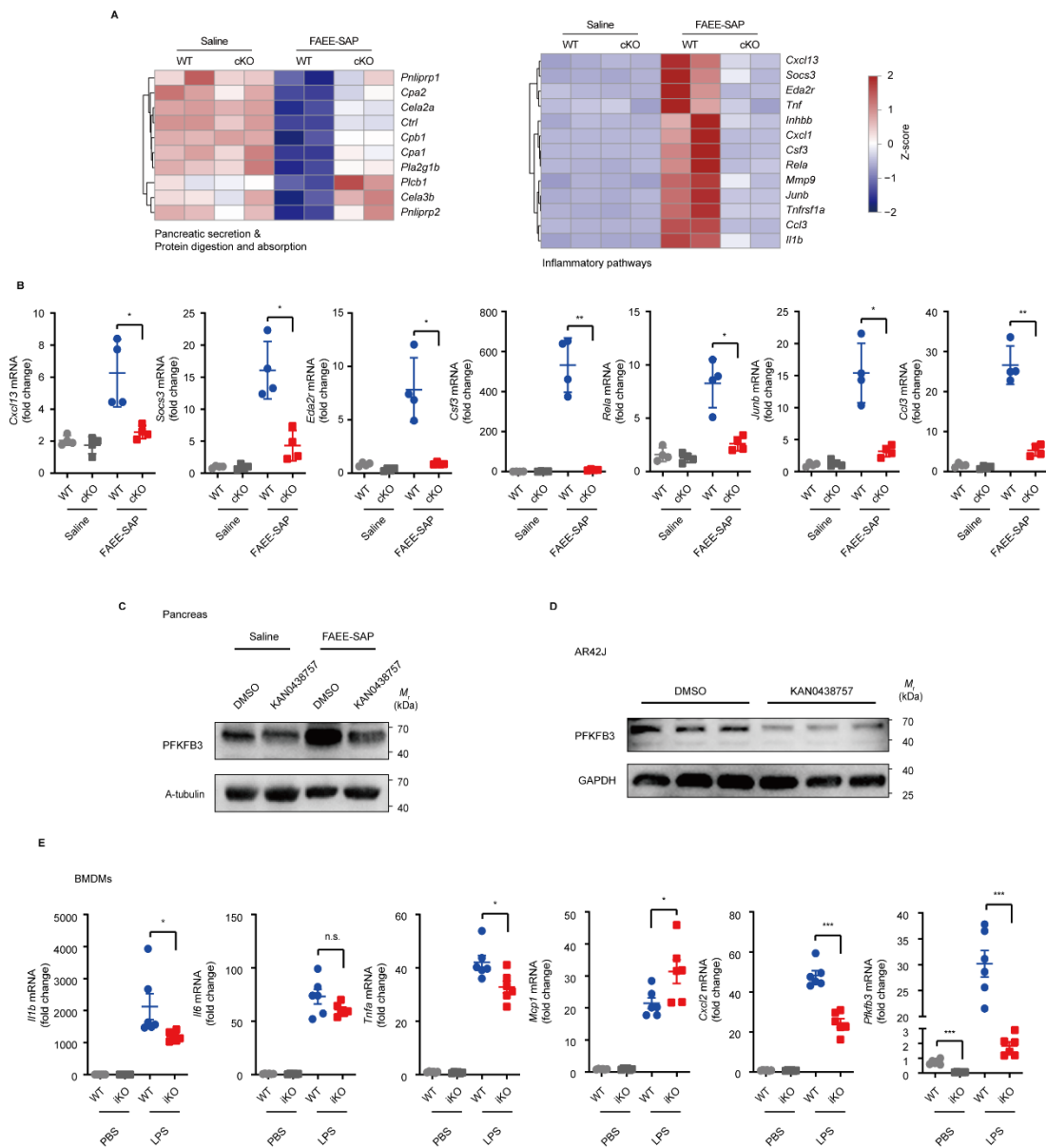


**Figure S11. Validation of sequencing data and protein level of pancreatic tissue. (A)** The heatmap shows the differentially expressed genes (DEGs) from **Fig. 5A** and **Fig. 5B**. FDR  $p < 0.05$  and fold change  $> 2$  or  $< -2$ . **(B)** The verification of representative differential expressed genes (DEGs) shown in **Fig.S11A** by RT-qPCR ( $n=4$ ). **(C-D)** The western blotting assay was used to verified the Inhibitory effect of KAN0438757 on PFKFB3. **(E)** Expression level of inflammatory markers when stimulated with LPS (100ng/ml,6h) in BMDMs derived from iKO and WT mice were detected using RT-qPCR ( $n=6$ ). All statistical analyses were done by unpaired student t-test and shown as mean  $\pm$  SD, \* $p < 0.05$ , \*\* $p < 0.01$ , \*\*\* $p < 0.001$ , n.s., not significant. Each experiment was done at least in triplicate.

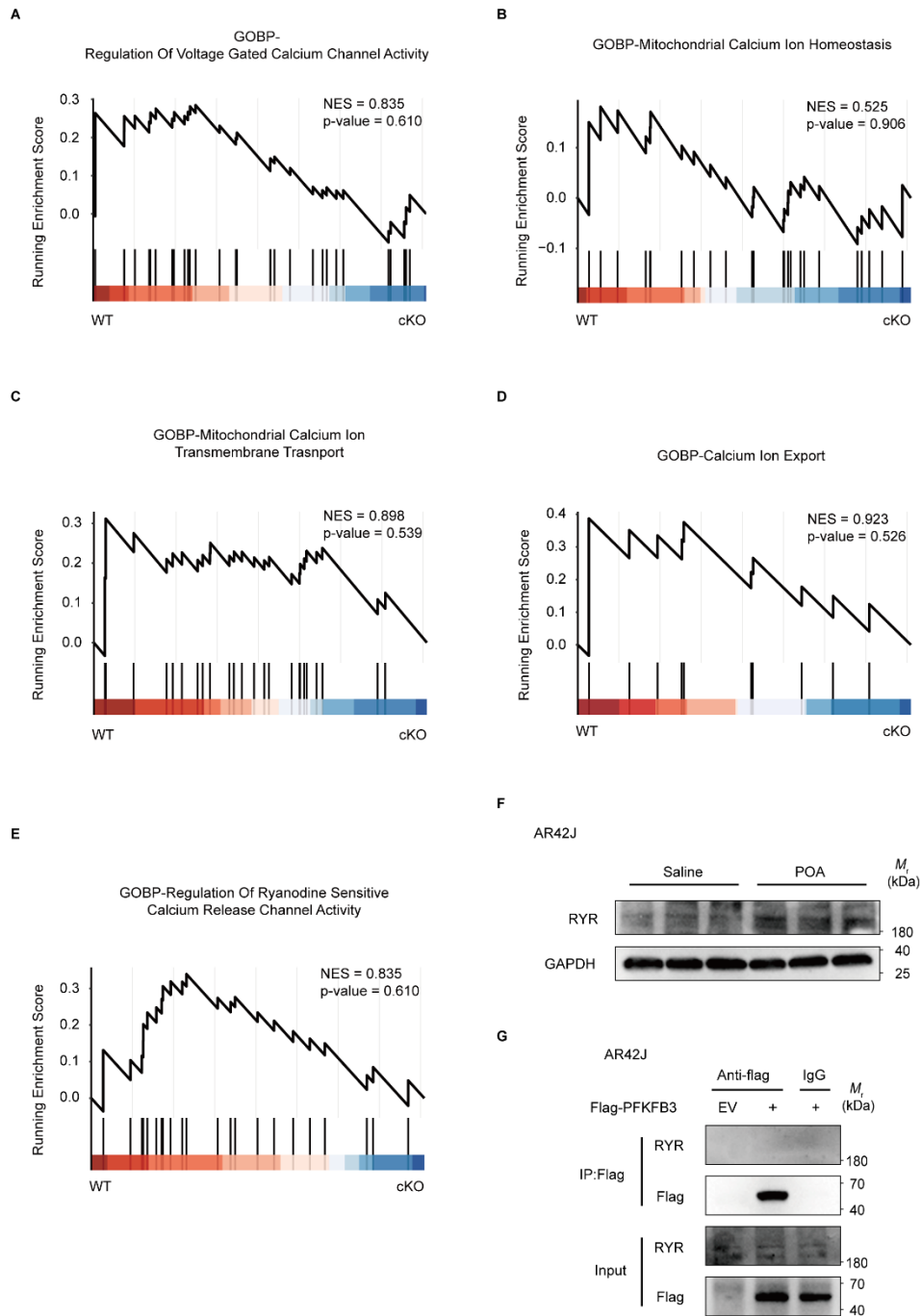


**Figure S12. Elimination of downstream targets of PFKFB3. (A-E)** The enrichment plot compared the transcriptome of cKO mice and WT mice in FAEE-SAP derived from the GSEA analysis. **(F)** RYR expression in AR42J cells stimulated with POA (300  $\mu$ M) was determined by Western blotting. **(G)** AR42J cells were transfected with full length Flag-PFKFB3 construct for co-IP analysis.

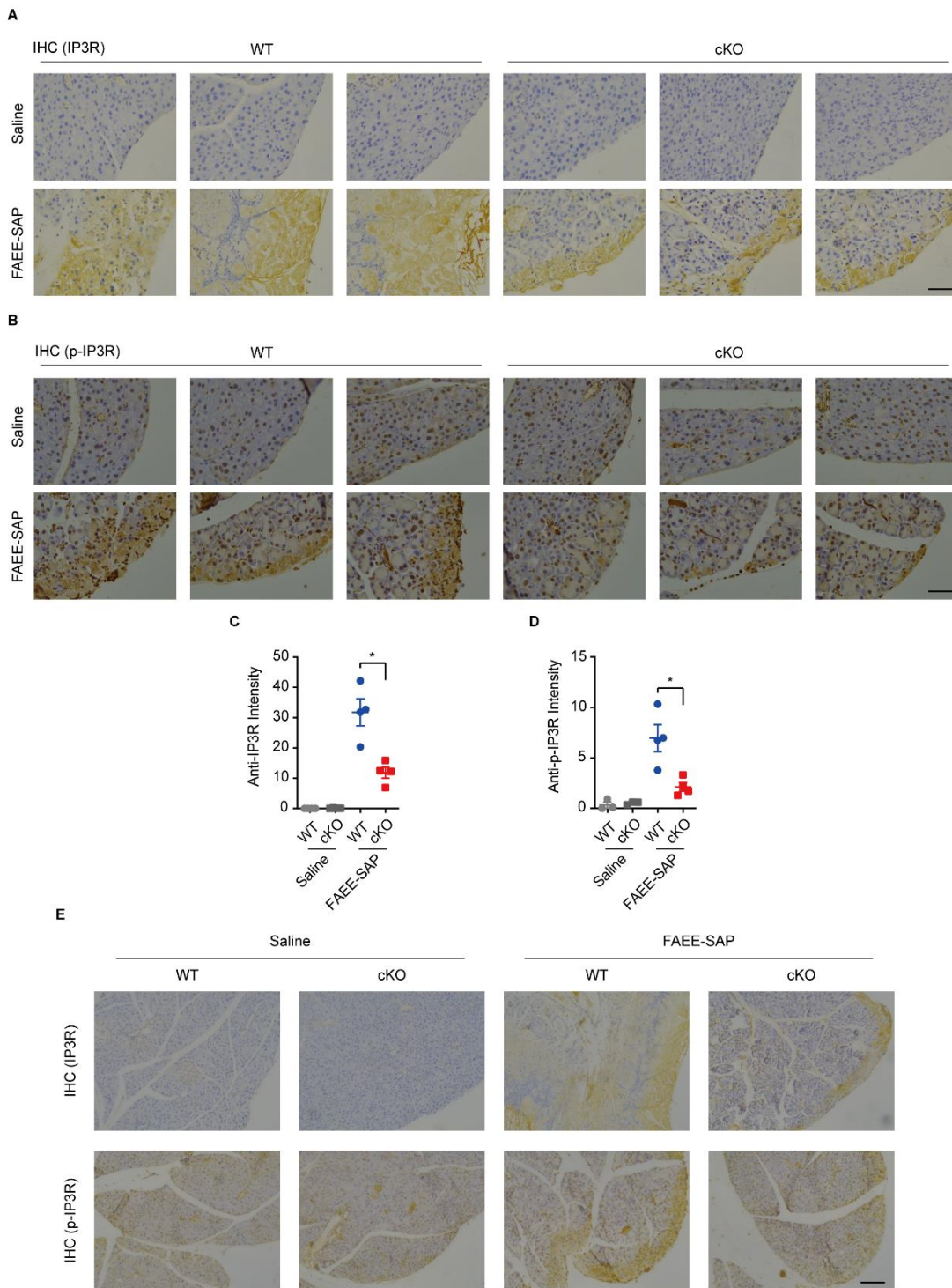


**Figure S13. Immunohistochemical analysis and quantification of IP3R (A, C) and p-IP3R (B, D) of injured and normal pancreas in WT mice and cKO mice. Scale bar, 50µm. Low magnification images (E) of IHC stain of injured and normal pancreas in WT mice and cKO mice. Scale bar, 100µm.**

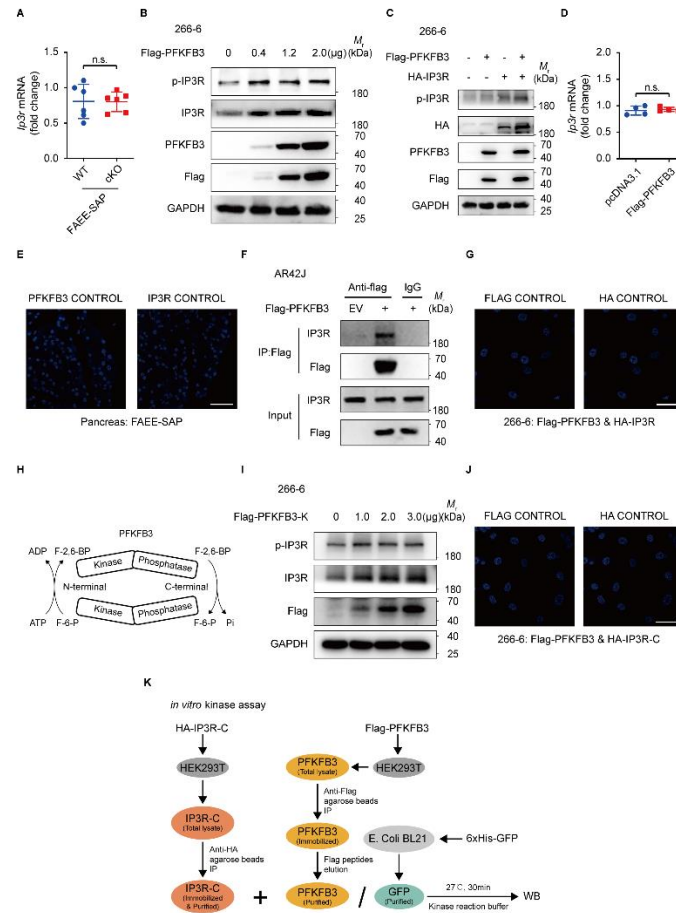


**Figure S14 Interaction between PFKFB3 and IP3R and its non-specific binding site.** (A) *Ip3r* mRNA expression of cKO mice and WT mice in the FAEE-SAP model (n=6). (B) 266-6 cells were transfected with increasing concentrations Flag-PFKFB3 construct, 24h post-transfection cells were harvested for Western blotting analysis. (C) Empty vector (pcDNA3.1), Flag-PFKFB3 and HA-IP3R constructs were co-transfected into 266-6 cells. After 24h, whole cell lysates were collected for Western blotting analysis. (D) mRNA expression of *Ip3r* in 266-6 cells transfected with empty vector (pcDNA3.1) and Flag-PFKFB3 constructs (n=4). (E) Antibody control of PLA assay in FAEE-SAP, scale bar, 40 $\mu$ m. (F) AR42J cells were transfected with full length Flag-PFKFB3 construct for co-IP analysis. (G) Antibody control of PLA assay in 266-6 cells co-transfected with Flag-PFKFB3 construct and HA-IP3R construct, scale bar, 40 $\mu$ m. (H) Schematic of the structural and functional information of PFKFB3. (I) Increasing concentrations Flag-PFKFB3-K were transfected into 266-6 cells for Western blotting analysis. (J) Antibody control of PLA assay in 266-6 cells co-transfected with Flag-PFKFB3 construct and HA-IP3R-C construct, scale bar, 40 $\mu$ m. (K) Schematic diagram indicates the principle of a cell-free system for *in vitro* kinase assay. All statistical analyses were done by unpaired student t-test and shown as mean  $\pm$  SD, n.s., not significant. Each experiment was done at least in triplicate.

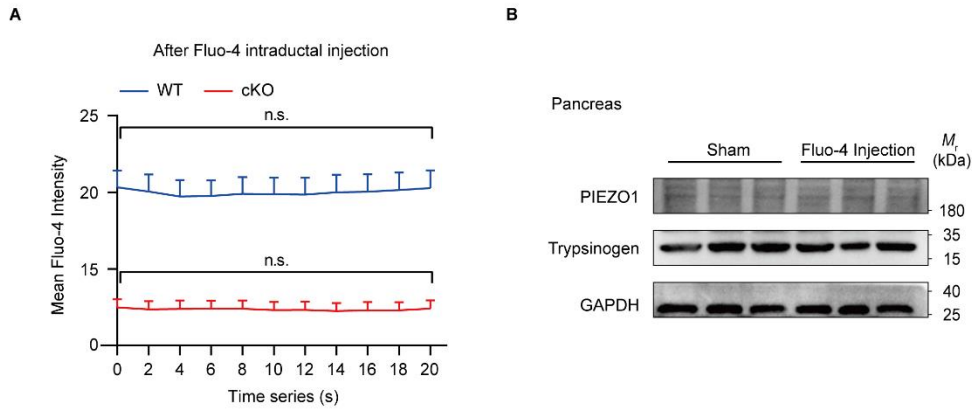


**Figure S15. (A) Representative traces of  $Ca^{2+}$  in acini after Fluo-4 intraductal injection. (B) The Western blotting analysis for protein collected from pancreas which intraductal injected with Fluo-4 for 20 mins. All statistical analyses were done by unpaired student t-test and shown as mean  $\pm$  SD, n.s., not significant. Each experiment was done at least in triplicate.**